Supporting information

Integration of phase change materials with multi-responsive halloysite nanotubes for efficient Pickering emulsification of high-viscosity oil

Limei Dong [a, b], Dan Zhang [a, b], Junfeng Li [a, b], Shichong Guo [a, b], Ying Xue [a, b], Zhining Wang [c], and Yiming Li [a, b, *]

[a] Frontiers Science Center for Deep Ocean Multispheres and Earth System/Key Laboratory of Marine Chemistry Theory and Technology, Ministry of Education, Ocean University of China, 266100, Qingdao, P.R. China

[b] College of Chemistry and Chemical Engineering, Ocean University of China, Qingdao, 266100, P.R. China

[c] Shandong Key Laboratory of Water Pollution Control and Resource Reuse, School of Environmental Science and Engineering, Shandong University, Qingdao 266237, P.R. China

[*] Corresponding author. Tel: 86 532 66782509. E-mail: liym@ouc.edu.cn (Y. M. Li)

Summary of Content

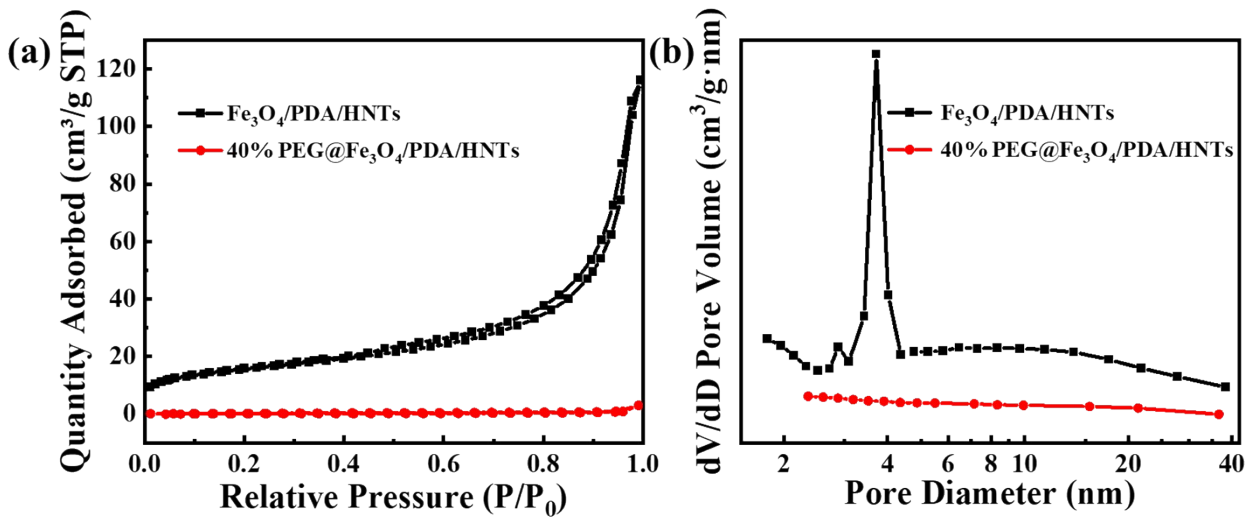

Fig. S1. (a) N_2 adsorption-desorption isotherms and (b) pore size distributions of Fe_3O_4/PDA/HNTs and 40% PEG@ Fe_3O_4/PDA/HNTs.

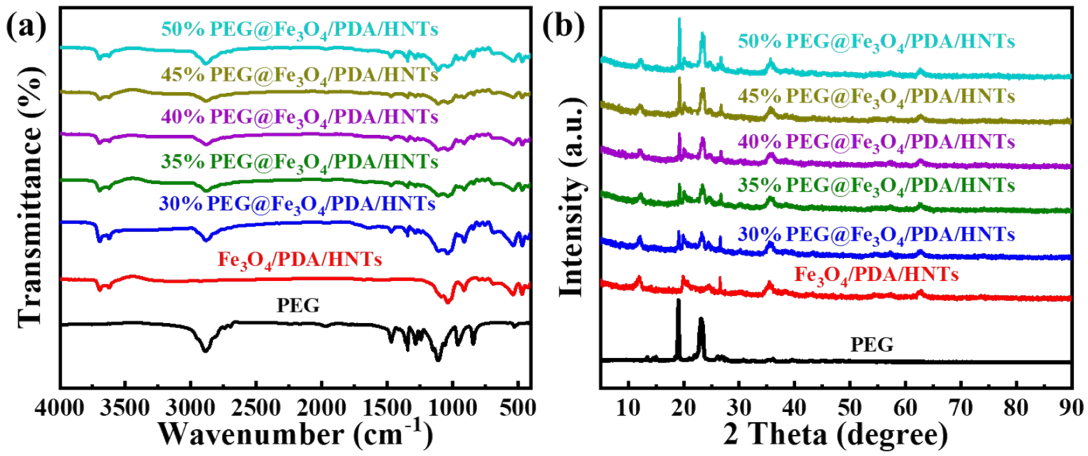

Fig. S2. (a) FTIR spectra and (b) XRD patterns of PEG@Fe_3O_4/PDA/HNTs with different PEG contents.

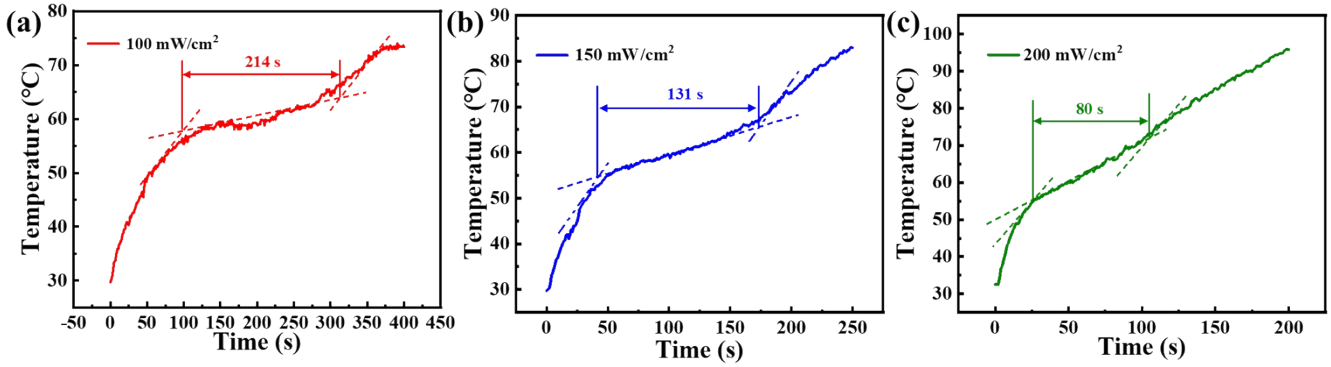

Fig. S3. Tangential method for determining the starting and terminating points of the phase change of 40% PEG@Fe_3O_4/PDA/HNTs at irradiation intensity of (a) 100 mW/cm^2, (b) 150 mW/cm^2 and (c) 200 mW/cm^2.

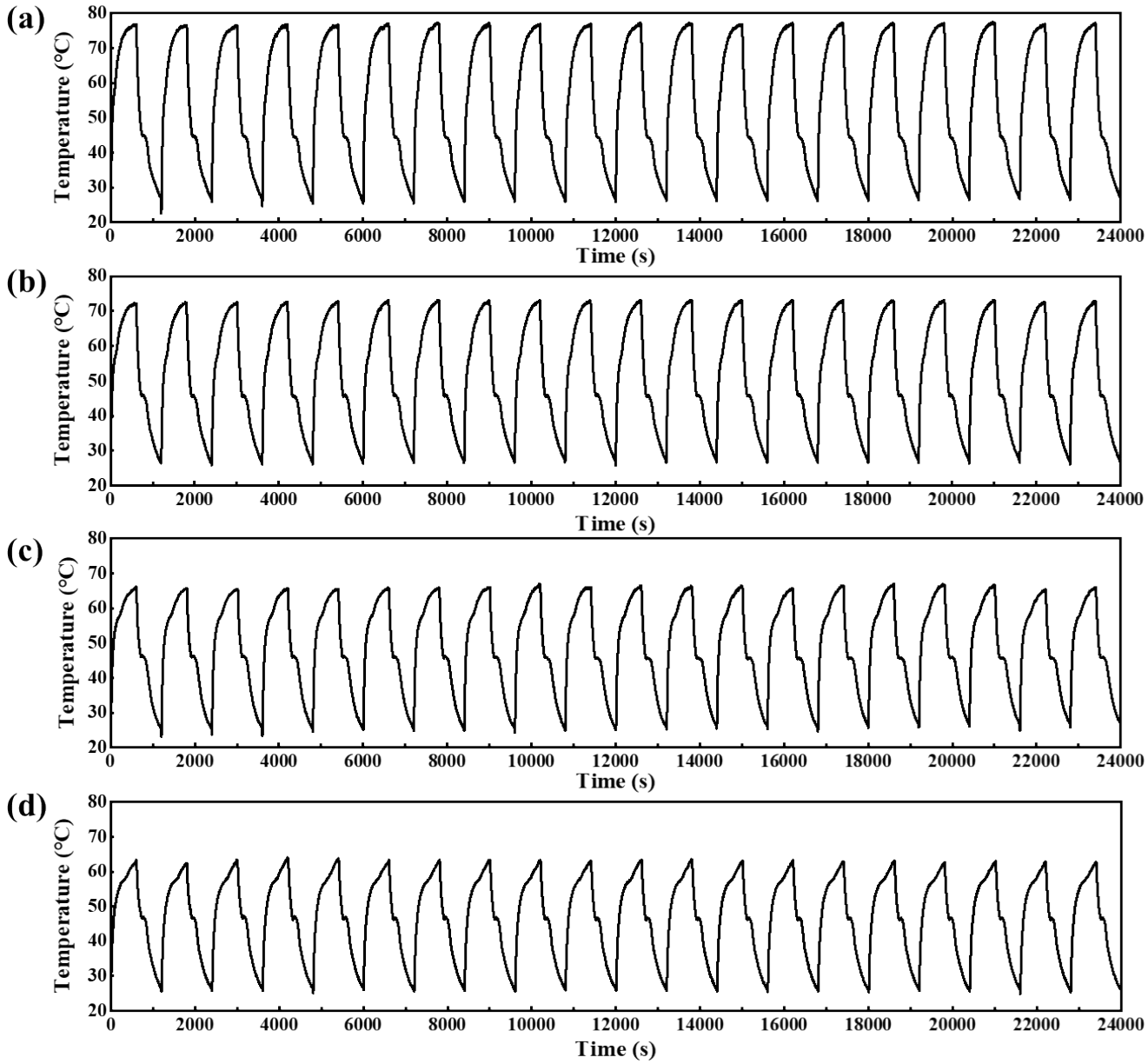

Fig. S4. The magnetic-thermal conversion cycling property of (a) 30% PEG@Fe_3O_4/PDA/HNTs, (b) 35% PEG@Fe_3O_4/PDA/HNTs, (c) 45% PEG@Fe_3O_4/PDA/HNTs and (d) 50% PEG@Fe_3O_4/PDA/HNTs.

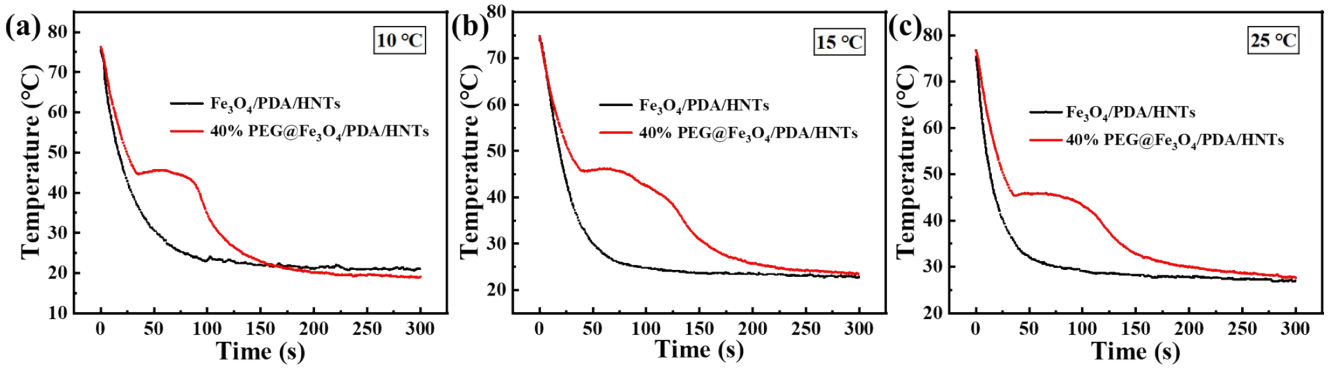

Fig. S5. The curves of temperature change with time after Fe_3O_4/PDA/HNTs and 40% PEG@Fe_3O_4/PDA/HNTs spread on the surface of the oil at (a)10 ℃, (b) 15 ℃ and (c) 25 ℃.

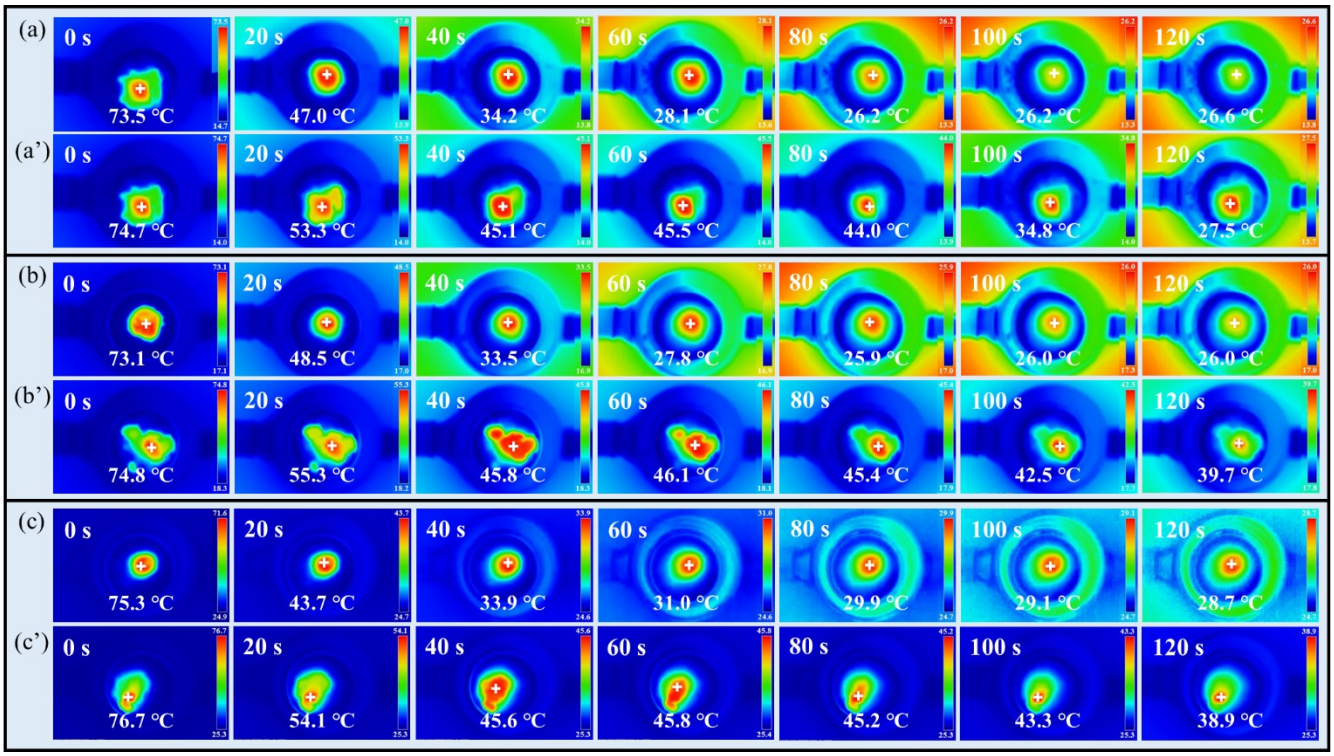

Fig. S6. The IR photographs after pre-heated (a, b, c) Fe_3O_4/PDA/HNTs and (a', b', c') 40% PEG@Fe_3O_4/PDA/HNTs spread on the surface of the oil at 10 ℃, 15 ℃ and 25 ℃, respectively.

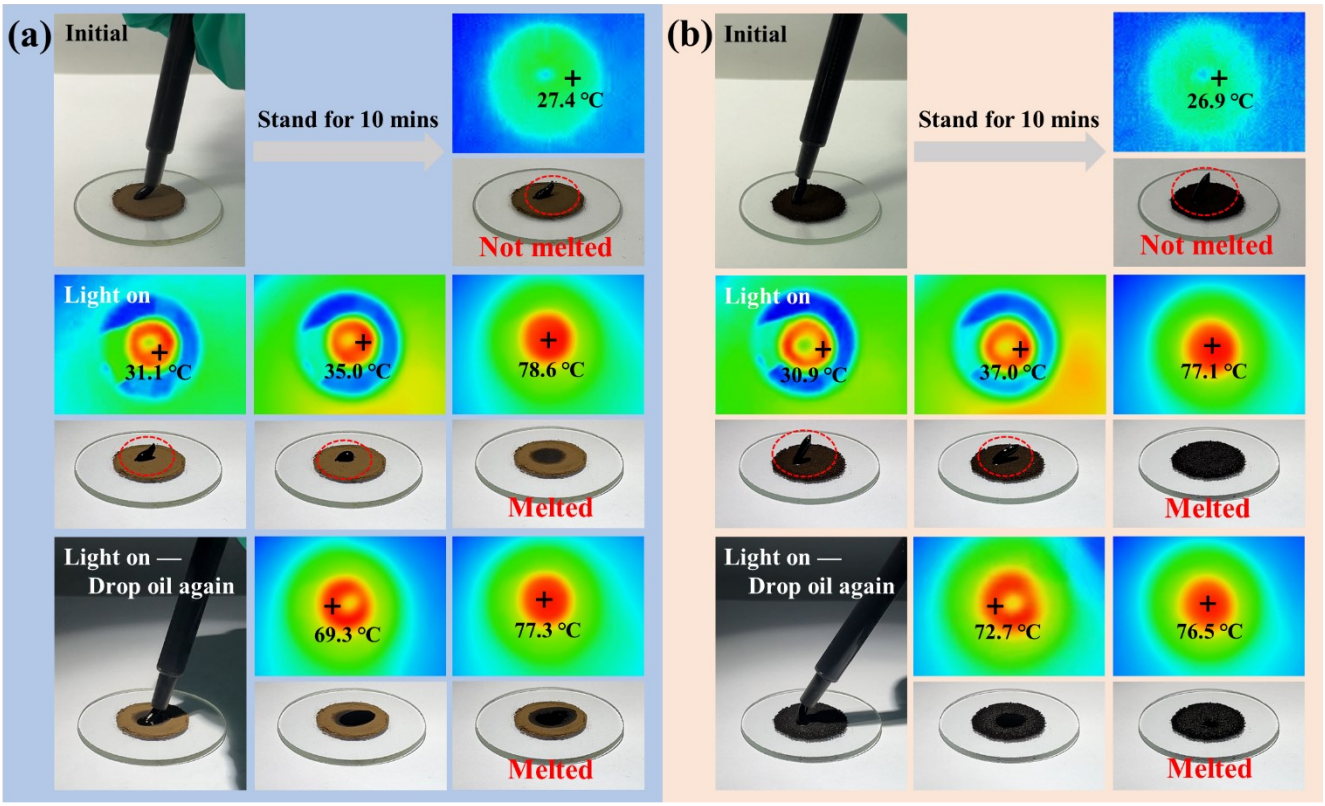

Fig. S7. Viscosity changes of high-viscosity oil droplets after in contact with (a) Fe_3O_4/PDA/HNTs and (b) 40% PEG@Fe_3O_4/PDA/HNTs under the light irradiation.

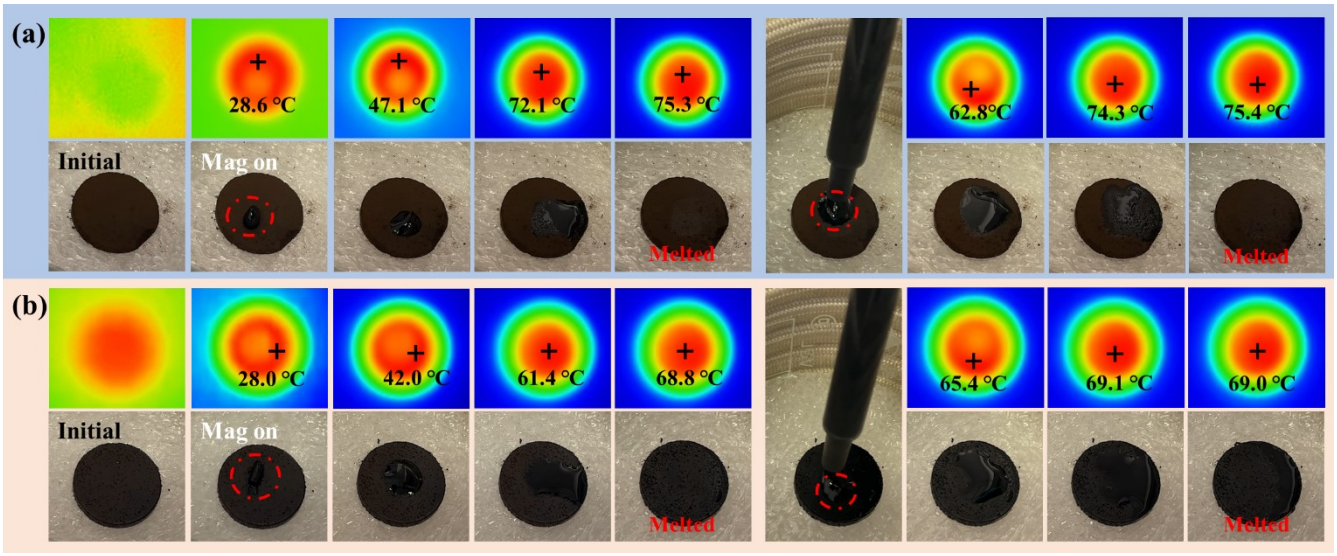

Fig. S8. Viscosity changes process of high-viscosity oil droplets in contact with (a) Fe_3O_4/PDA/HNTs and (b) 40% PEG@Fe_3O_4/PDA/HNTs under an alternating magnetic field.

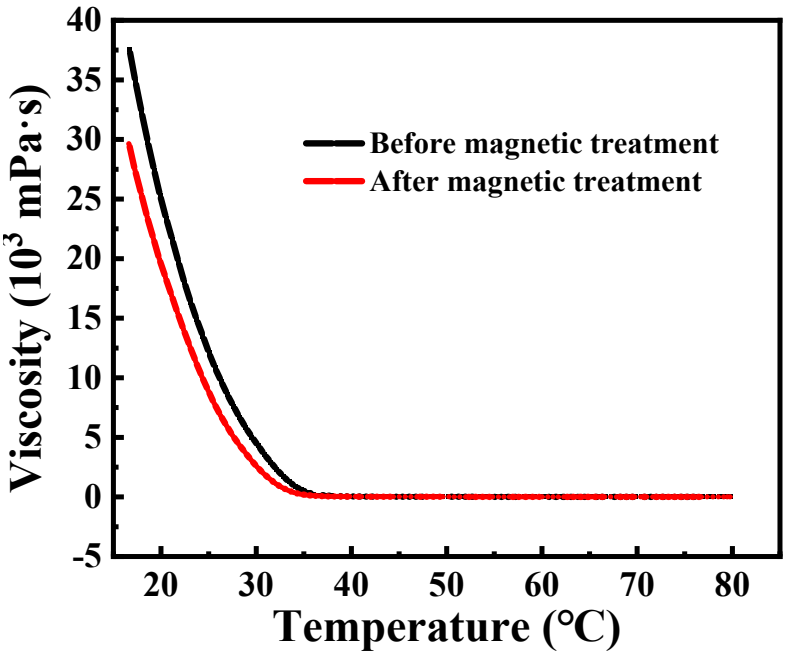

Fig. S9. The comparison of viscosity-temperature curves before and after magnetization.

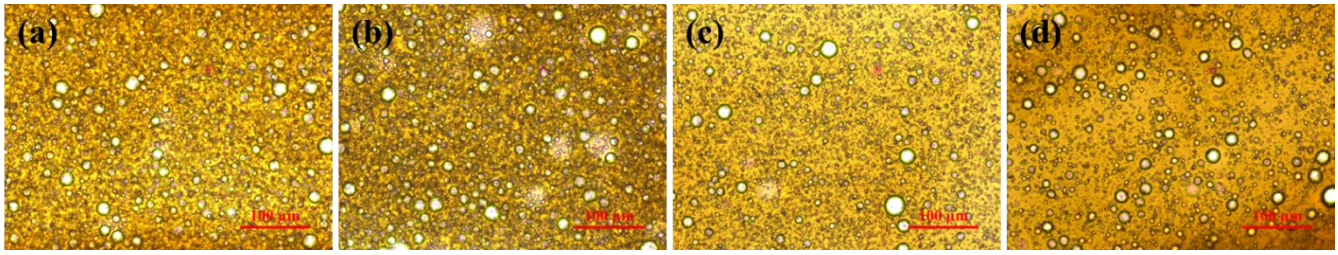

Fig. S10. Optical microscopy images of emulsions without emulsifier at the oil to water volume ratio of (a) 1:4, (b) 1:6, (c) 1:9, (d) 1:12.

Table S1 Thermal properties of pure PEG and PEG@Fe_3O_4/PDA/HNTs composites

Samples	Melting process		Solidifying process	
	ΔH_m (J/g)	T_m (°C)	ΔH_c (J/g)	T_c (°C)
Pure PEG	180.61	59.17	167.21	48.41
30% PEG@Fe_3O_4/PDA/HNT	51.28	55.66	43.08	41.76
35% PEG@Fe_3O_4/PDA/HNT	59.34	54.86	49.13	42.70
40% PEG@Fe_3O_4/PDA/HNT	68.24	55.93	57.84	41.54
45% PEG@Fe_3O_4/PDA/HNT	78.18	56.33	67.14	43.00
50% PEG@Fe_3O_4/PDA/HNT	88.57	57.21	77.77	44.31

Table S2 Thermal properties of 40% PEG@Fe_3O_4/PDA/HNTs composites before and after cycling.

Samples	Melting process		Solidifying process	
	ΔH_m (J/g)	T_m (°C)	ΔH_c (J/g)	T_c (°C)
Before cycles	68.24	55.93	57.84	41.54
50 cycles	69.89	56.46	56.72	41.98
100 cycles	70.44	56.36	59.02	44.30

Table S3 Comparisons of thermal conductivities between this research and reported results.

PCMs	Support	Thermal conductivity W/ (m·K)	Thermal conductivity enhancement (%)	Refs.
PEG 6000	Cu/SiO_2	0.41	38.1	1
PEG 6000	SiO_2-PDA/Ag	0.50	70.4	2
PEG 6000	SiO_2-Al_2O_3	0.42	41.1	3
PEG 6000	Fe_3O_4-GO	0.38	52.0	4
PEG 6000	Fe_3O_4/PDA/HNTs	0.78	130.0	This work

Table S4 Comparisons of photothermal conversion performance between this research and reported results.

Samples	Irradiation intensity (mW/cm^2)	Temperature (℃)	Photothermal conversion efficiency (%)	Refs.
Pn@ND/MF microPCMs [a]	-	73.0	64.7	5
ODE microcapsules [b]	500.0	39.4	42.8	6
HPC-PW [c]	200.0	70.0	31.0	7
FCA [d]	200.0	47.0	60.6	8
PEG@MCHS [e]	150.0	80.9	58.0	9
PEG@Fe_3O_4/PDA/HNTs	100.0	80.9	69.2	This work

[a] Pn@ND/MF microPCMs: paraffin@nanodiamond/melamine formaldehyde microencapsulated phase-change materials; [b] ODE microcapsules: n-Octadecane with titanium dioxide nanoparticle-doped styrene-divinylbenzene copolymer; [c] HPC: hierarchical porous carbon; [d] FCA: Fe-doped carbon aerogel; [e] MCHS: mesoporous carbon hollow spheres.

Table S5 Comparisons of magnetic-thermal conversion performance and magnetic-thermal conversion performance between this research and reported results.

Samples	Irradiation intensity (mW/cm^2)	Temperature (℃)	Input alternating current (A)	Temperature (℃)	Refs.
LA/CKF@Fe_3O_4 [a]	100.0	60.0	-	50.0	10
MXene@PDA@PPEE [b]	-	87.0	12.4	75.0	11
MXene@Fe_3O_4-MA-PU [c]	150.0	75.0	10.0	70.0	12
FCA	200.0	47.0	12.0	60.0	8
PEG@Fe_3O_4/PDA/HNTs	100.0	80.9	8.0	68.5	This work

[a] LA/CKF: lauric acid/carbonized kapok fiber aerogel; [b] PPEE: PEG@PDA@EPDM/EG; [c] MA: myristic acid.

References

1 B. Tang, M. Qiu and S. Zhang, *Sol. Energy Mater. Sol. Cells*, 2012, **105**, 242-248.
2 J. Li, X. Hu, C. Zhang, W. Luo and X. Jiang, *Renew. Energ.*, 2021, **178**, 118-127.
3 B. Tang, C. Wu, M. Qiu, X. Zhang and S. Zhang, *Mater. Chem. Phys.*, 2014, **144**, 162-167.
4 L. Liu, J. Hu, X. Fan, Y. Zhang, S. Zhang and B. Tang, *Chem. Eng. J.*, 2021, **426**, 130789.
5 L. Xu, Q. Zhao, Y. Li, F. He, Y. Zhou, R. He, J. Fan, K. Zhang and W. Yang, *Ind. Eng. Chem. Res.*, 2020, **59**, 21736−21744.
6 K. Zhao, Z. Guo, J. Wang and H. X. Xie, *Sol. Energy*, 2023, **254**, 73-87.
7 K. Sun, Y. Kou, Y. Zhang, T. Liu and Q. Shi, *ACS Sustainable Chem. Eng.*, 2020, **8**, 3445-3453.
8 K. Sun, Y. Kou, H. Dong, S. Ye, D. Zhao, J. Liu and Q. Shi, *J. Mater. Chem. A*, 2021, **9**, 1213-1220.
9 L. Dong, Y. Li, J. Li, Y. Guan, X. Chen, D. Zhang and Z. Wang, *J. Hazard. Mater.*, 2023, **451**, 131112.
10 S. Song, H. Ai, W. Zhu, L. Lv, R. Feng and L. Dong, *Composites, Part B*, 2021, **226**, 109330.
11 X. Hu, B. Quan, B. Ai, M. Sheng, S. Liu, X. Huang, H. Wu, L. Xiang and J. Qu, *J. Mater. Chem. A*, 2023, **11**, 16138.
12 Y. Gao, Z. Tang, X. Chen, J. Yan, Y. Jiang, J. Xu, Z. Tao, L. Wang, Z. Liu and G. Wang, *Aggregate*, 2022, **4**, e248.